

REMOTE SENSING ESTIMATION OF LITTERFALL DYNAMICS

Hsueh-Ching Wang^{1*}, Huai-Tse Yang² and Cho-Ying Huang³

¹ PhD student, Department of Geography, National Taiwan University, No. 1, Sec. 4, Roosevelt Road, Taipei, Taiwan; Tel +886-2-33663733;
E-mail: hsuehching.wang@gmail.com

² Undergraduate student, Department of Forestry and Resource Conservation, National Taiwan University, No. 1, Sec. 4, Roosevelt Road, Taipei, Taiwan; Tel +886-2-33663733;
E-mail: b97605078@ntu.edu.tw

³ Assistant Professor, Department of Geography, National Taiwan University, No. 1, Sec. 4, Roosevelt Road, Taipei, Taiwan; Tel +886-2-33663733;
E-mail: choying@ntu.edu.tw

KEY WORDS: Litterfall, Remote Sensing, MODIS, Landsat, spectral mixture analysis

ABSTRACT: Litterfall represents the major losses of aboveground carbon and nutrients to forest floors, which are pivotal components in terrestrial biogeochemical cycles. It is also an indicator to assess the impacts of perturbations on forest ecosystems such as tropical cyclones and insect infestation. The objective of this study is to conduct a large scale research to estimate the litterfall by combining field observations and estimates from multi-scale remote sensing techniques in a subtropical forest in Taiwan. Litterfall traps across a wide range of topo-edaphic gradients were installed and periodically collected data in Lienhuachi experimental forest (n = 18) and in Chilan mountain (n = 10). Enhance vegetation index (EVI), photochemical reflectance index (PRI) and photosynthetic vegetation (PV) were used to estimate time-series dynamics of litterfall from Landsat TM/ETM+ and MODIS images. Results showed that there had no significant correlations between litterfall data and the differences of monthly EVI (r = -0.17), monthly mean EVI (r = 0.08) and sPRI (r = 0.10). But there was a tricky positive relationship between Δ PV and litterfall (r = 0.63, p-value = 0.012). If the values of litterfall induced by typhoon were took out, the relationship between Δ PV and litterfall was not significant (r = -0.25, p-value > 0.05). No significant correlations between vegetation indices and litterfall could be due to that the study sites were located at evergreen broadleaf and conifer forests where the seasonal dynamics of EVI (0.30 – 0.57) and sPRI (0.42 – 0.51) were small compared to deciduous forest, and it was difficult for remote sensing technique to capture the high variable dynamics of litterfall (90 - 1800 kg/ha). If the changes of vegetation phenology were not significant, the signal of litterfall will be easily mixed with noises in the images. Based on preliminary observation, finding a more sensitive index to capture the slight dynamics of litterfall and vegetation phenology is important in the future.

1. INTRODUCTION

Litterfall is the major pathway to return the nutrients and dead organic matter from plant community to soil surface, which play an important role on maintenance of soil fertility and pivotal components in terrestrial biogeochemical cycles (Barlow et al. 2007; Liao et al. 2006). Litterfall is also an indicator to assess the impacts of perturbations on forest ecosystems such as tropical cyclones and insect infestation (Lin et al. 2003; Lovett et al. 2002). Therefore, it is important to assess temporal dynamics of litterfall, which makes it possible for the regional monitoring of biogeochemistry in forest ecosystems.

Most estimates of litterfall are from field inventory using traps (Barlow et al. 2007; Lin et al. 2003; Whigham et al. 1991). Litterfall sampling traps are setup to collect litterfall at specified points in a study area. Depending on experimental design, researchers collect litter falling from trees and other vegetation over a specified period of time. Litterfall was taken to the laboratory to calculate dry biomass and analyze nutrient contents. This sampling method has been widely used to quantify canopy dynamics over seasons or understand responses to ecosystem disturbances at a specified site.

Except to *in-situ* litterfall traps, modeling of litterfall is another method to estimate litterfall. However modeling of litterfall is difficult due to high variations in litterfall dynamics, and there are fewer studies focused on this field. Vegetation senescence is highly related to climate and stand characteristics, which

are the major factors to model litterfall (Brown and Lugo 1982; Starr et al. 2005). Brown and Lugo (1982) collected a lot of field litterfall data from tropical and subtropical literatures to model litterfall using the ratio of temperature to precipitation (T/P) as an index, and found that T/P is a suitable index to predict litterfall productions. Except for climate factors, Starr et al. (2005) also considered latitude and stand characteristics (e.g. stand basal area, tree height and stem density) as indices, and use multiple regression models to estimate annual litterfall production. Staelens et al. (2003) developed spatial explicit models to estimate the effects of wind on litterfall using the tree diameter as an index, and to promote the understanding of small-scale litterfall processes.

However, impacts of tropical cyclones or insect infestation often affect relatively wide regions, and might result in substantial variations of litterfall according to different vegetation characteristics at various landscapes. Regardless of using field data or litterfall models, it is difficult to estimate litterfall over wide landscape regions. Large-scale remote sensing technique might be a potential method to estimate regional litterfall dynamics. However, using satellite images to estimate litterfall is absent until now, while there have been some literatures to estimate coarse woody debris derived by tropical cyclones (Chambers et al. 2007; West et al. 2011). Compared to substantial carbon storage in coarse woody debris, litterfall is a major pathway to return nutrients into soil surface for vegetation growth, microbial production and soil fertility (Chapin et al. 2002). Therefore, using satellite images to estimate litterfall over landscape scale could be useful to understand vegetation phenology and nutrients dynamics.

Based upon the aforementioned discussion, developing a relationship between field litterfall data and remote sensing indices is important. According to literatures of litterfall modeling, temperature, precipitation and stand characteristics could be critical factors to estimate litterfall (Brown and Lugo 1982; Starr et al. 2005). Many studies have demonstrated that remote sensing indices such as enhanced vegetation index (EVI), photosynthetic vegetation (PV) and photochemical reflectance index (PRI) are useful predictors related to vegetation phenology and stand characteristics (Asner et al. 2003; Chambers et al. 2007; DeFries 2008; Froelking et al. 2009; Garbulsky et al. 2008). Therefore, we will use these remote sensing indices to estimate litterfall. This integration between remote sensing index and litterfall field data will be an important approach to understand large-scale dynamics of ecosystem.

2. MATERIALS AND METHOD

2.1 Site description

The objective of study is to integrate field and satellite observations to estimate litterfall in a subtropical forest in Taiwan (23°54' N, 121°54' E) (Fig. 1). Litterfall traps across a wide range of topo-edaphic gradients were installed and periodically collected data in Chilan mountain (n = 10) during August 2003 to December 2004 (Chu 2005) and in Lienhuachi experimental forest (n = 18) during May 2008 to April 2009 (Wang 2009). *Chamaecyparis obtusa* var. *formosana* is the dominant species in Chilan Mountain and the elevation is across an range of 1400-1800 m in northern Taiwan. The climate is temperate and humid, and the mean annual temperature is 13°C. The mean annual precipitation is 4005 mm and varies from 2000 mm to 5000 mm depending on the frequency and intensity of typhoons in the summer (Chang et al. 2006). Lienhuach experimental forest is located at middle of Taiwan and the elevation is across 550-950 m. Climate is warm and humid, but there is significant dry and wet season. The mean annual temperature is 20°C and the mean annual precipitation is 2230 mm. Subtropical broadleaf forest is the dominant vegetation in Lienhuach experimental forest, but there have some coniferous plantation forests such as *Cunninghamia lanceolata* and *Calocedrus macrolepis* var. *formosana* (Wang 2009).

2.2 Remote sensed data acquisition and processes

The EVI and PRI were characterized using a high temporal resolution Terra Moderate Resolution Imaging Spectroradiometer (MODIS) image with 12-bit in 36 spectral bands ranging in wavelength from 0.4 μm to 14.4 μm . The PV was characterized using a high spatial resolution Landsat TM or ETM+ images with 8-bit in 7 and 8 spectral bands for TM and ETM+, respectively. The spectral bands are ranging in wavelength from 0.45 μm to 12.5 μm . Data acquisition and process are different according to EVI, PRI, PV indices, and the specific processes are the following (Fig. 2):

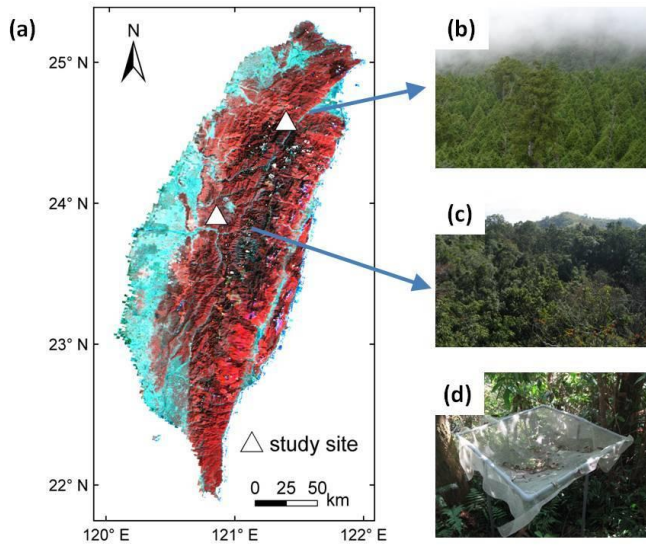


Fig. 1 (a) A multispectral MODIS image of the study site in Taiwan. (b) The *Chamaecyparis obtusa* var. *formosana* coniferous forest in Chilan Mountain. (c) The broadleaf and mixed forests in Lienhuachi. (d) The 1m × 1m litterfall traps were setup to collect litterfall.

2.2.1 Enhanced vegetation index

The 16-days MODIS surface reflectance data (MOD13Q1) with 250 m spatial resolution in 2000-2010 were downloaded from the NASA website to estimate the greenness of forest. The EVI enhances vegetation signals that would not saturate in a highly vegetated area, and it is not sensitive to noises from the soil background and atmosphere profile that would contaminate satellite signals (Huete et al. 2002). The model for the EVI is:

$$EVI = G * (\rho_{NIR} - \rho_{red}) / (\rho_{NIR} + C_1 \rho_{red} - C_2 \rho_{blue} + L) \quad (1)$$

where ρ is surface reflectance (unitless) and the subscripts indicate NIR, red and blue bands. Note that G is a gain factor, C_1 and C_2 are atmosphere resistance correction coefficients, and L is the canopy background brightness correction factor. The coefficients adopted in the Eq. 1 were $G = 2.5$, $C_1 = 6$, $C_2 = 7.5$, and $L = 1$. EVI values of temporal dynamics will be compared with field litterfall data.

2.2.2 Photochemical reflectance index

The daily MODIS reflectance data (Terra L1b MOD021KM) in 2000-2010 were downloaded from the NASA website. The MODIS bands 11 (526–536 nm) and 12 (546–556 nm) with 1 km spatial resolution were used to calculate the PRI. Because the atmospheric effects on bands 11 and 12 are similar and PRI would not be affected by atmospheric correction (Drolet et al. 2005; Garbulsky et al. 2008), this study will use downloaded bands 11 and 12 for PRI calculation. The model for the PRI is:

$$PRI = (\text{band 11} - \text{band 12}) / (\text{band 11} + \text{band 12}) \quad (2)$$

$$\text{band 11} = 526\text{--}536 \text{ nm}; \text{band 12} = 546\text{--}556 \text{ nm}$$

The PRI is a normalized index and the value is a range of -1 to 1. To obtain only positive values, PRI was scaled to an adjusted range of 0 to 1 termed as sPRI (Rahman et al. 2001).

$$sPRI = \text{sPRI} = (PRI + 1) / 2 \quad (3)$$

2.2.3 Photosynthetic vegetation

Landsat TM and ETM+ images with 30 m spatial resolution were downloaded from USGS glovis website and atmospheric correction was applied to images. This study used reported standard conversion coefficients to compute at-sensor spectral radiance ($Wm^{-2}m^{-1}sr^{-1}$) from the raw digital numbers. For the standard atmosphere correction, this study used the Atmospheric CORrection Now (ACORN) v. 6b (ImSpec LLC, Palmdale, CA, USA) software to remove the atmosphere profile from the image and convert radiance to surface reflectance. To reduce effects of cloud cover, this study will use automated cloud-cover assessment algorithm to remove cloud (Irish et al. 2006).

After atmospheric correction, images will be used for spectral mixture analysis using Automated Monte Carlo unmixing (AutoMCU) model in this study (Asner and Lobell 2000). Monte Carlo simulation is used to extract endmembers (photosynthetic vegetation, non-photosynthetic vegetation and soil) in

each pixel, and many PV, NPV and soil endmembers are randomly selected for simulations. Endmembers of NPV and soil from *in situ* litter and soil collected in Taiwan were measured using portable spectroradiometer, while endmember of PV was collected by Hyperion images. Owing to difficult to separate NPV and soil in Landsat TM and ETM+ images, NPV and PV endmembers were combined for analysis. After simulating, we can get %PV and %NPV+soil in each pixel, which will be used to estimate litterfall and compare with field inventory.

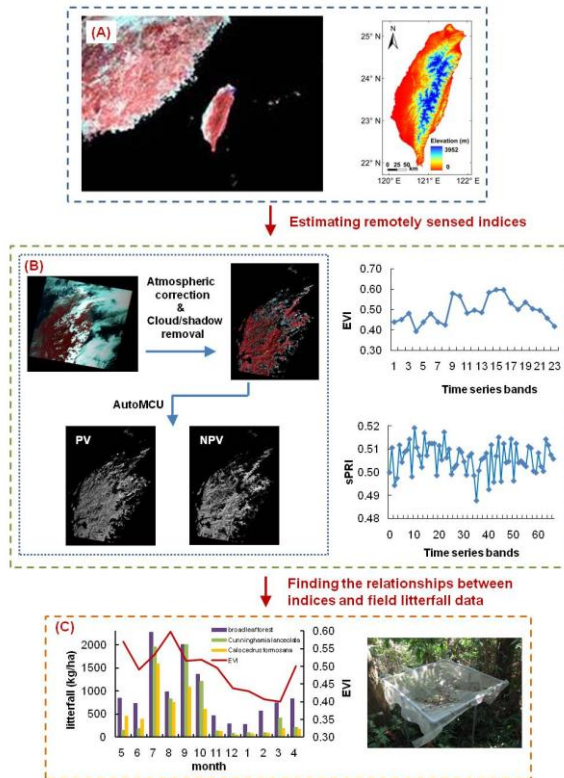
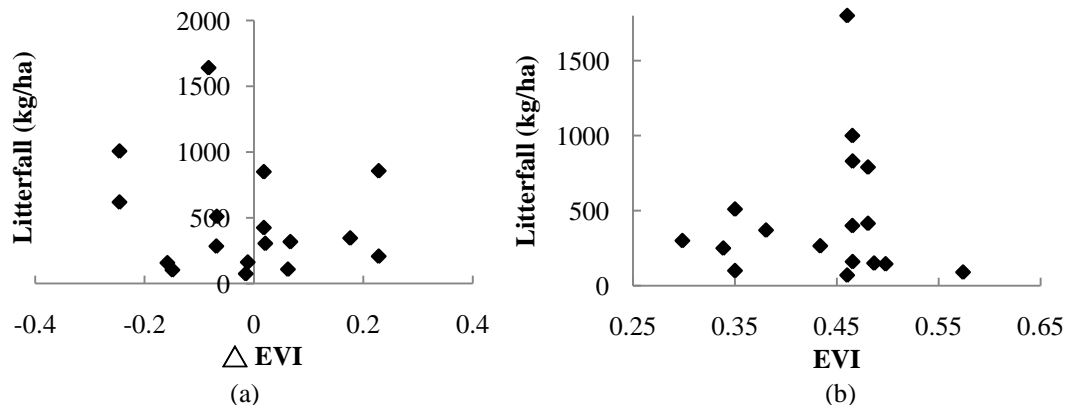


Fig. 2 The workflow of this study. (A) MODIS 16-days satellite images with 250m spatial resolution. ASTER Global Digital Elevation Model (GDEM) topography with 30m spatial resolution. (B) Landsat imagery with atmospheric correction and cloud/shadow removal. After pre-processing of images, AutoMCU for spectral mixture analysis was used to separate the proportions of PV and NPV. Time series distributions of EVI and sPRI from MODIS images. (C) Field litterfall data and traps for collecting litterfall.

3. RESULTS AND DISCUSSION

Results showed that there had no significant correlations between field litterfall data and the difference of monthly EVI (EVI in end of month – EVI in beginning of month = Δ EVI) ($r = -0.17$, p -value > 0.05), monthly mean EVI ($r = 0.08$, p -value > 0.05) and sPRI ($r = 0.10$, p -value > 0.05) (Fig. 3). It meant that it was difficult to use the patterns of Δ EVI, mean EVI and sPRI to capture the seasonal dynamics of litterfall. The study sites were located at evergreen broadleaf and conifer forests where the seasonal dynamics of EVI (0.30 – 0.57) and sPRI (0.42 – 0.51) were small compared to deciduous forest, and remote sensing indices were difficult to response high variable dynamics of litterfall (90 - 1800 kg/ha). The poor relationships might also be due to coarse spatial resolution (250 m and 1 km) resulting in spectral mixture effects from many surface endmembers mixed in one pixel, and the detailed dynamic of vegetation phenology such as litterfall was easily mixed and disappeared.



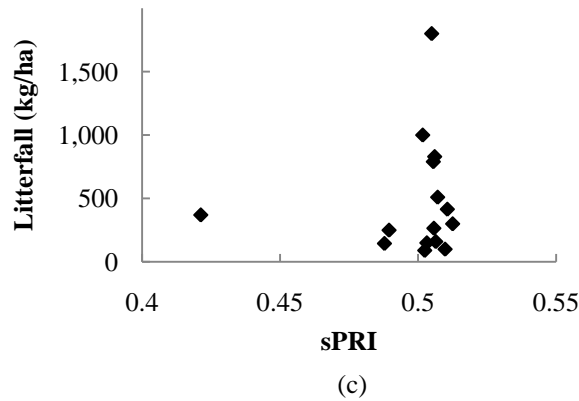


Fig. 3 (a) There was no significant correlation between litterfall and Δ EVI (EVI in end of month – EVI in beginning of month) ($r = -0.17$, p -value > 0.05). (b) The relationship between litterfall and mean EVI for each month was not significant ($r = 0.08$, p -value > 0.05). (c) There was no significant relationship between litterfall and sPRI ($r = 0.10$, p -value > 0.05).

To avoid the effects of mixed spectral, we used the spectral mixture analysis to separate PV, NPV and soil endmembers to capture the detailed dynamic of vegetation phenology. There was a strong correlation ($r = 0.63$, p -value = 0.012) between field litterfall and the difference of PV (Δ PV) within two consecutive images through time (Fig. 4). However, there was a tricky positive relationship between Δ PV and litterfall. High values of Δ PV and litterfall during the growing season (April-September) may be due to leaf expansion and tropical cyclones, respectively, leading to difficultly separate the contributions. If the values of litterfall induced by typhoon were took out, the relationship between Δ PV and litterfall was not significant ($r = -0.25$, p -value > 0.05) (Fig. 4). Difficult to separate the leaf expansion and tropical cyclones was due to that revisit interval of Landsat satellite was long (16 days) and it was difficult to find suitable images with less cloud cover in subtropical/tropical regions. Long revisit interval and less suitable images resulted in mixed effects of leaf growth and tropical cyclones from very long interval of images. Therefore, to avoid this mixed effect, the interval of images should be shorter to capture the changes of vegetation phenology or effects of tropical cyclones immediately, especially in evergreen subtropical/tropical forests.

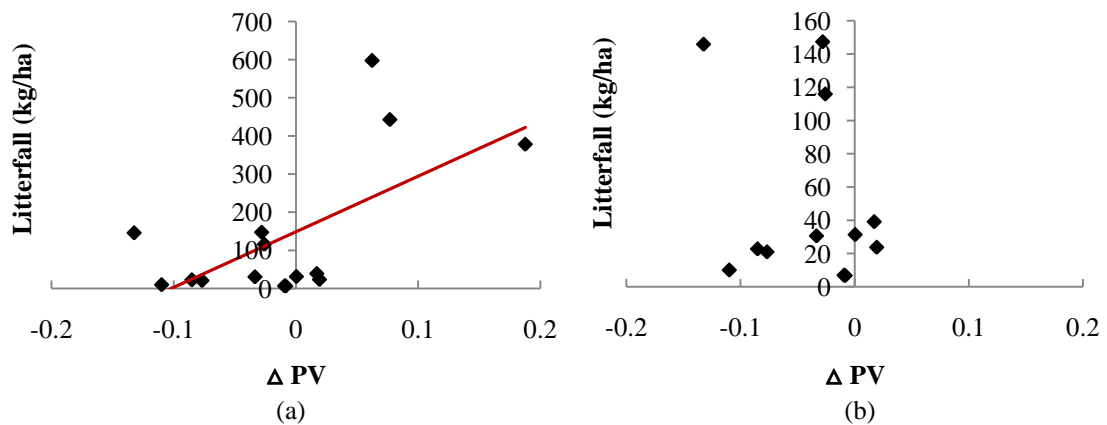


Fig. 4 (a) The relationship between litterfall and Δ PV (PV in later images – PV in earlier images) had a significant positive correlation ($r = 0.63$, p -value = 0.012). (b) However, if we remove the images in typhoon season, there was no significant correlation between them ($r = -0.25$, p -value > 0.05).

No significant correlations between vegetation indices and litterfall could be due to that the pattern of vegetation phenology was not significant seasonality, and the signal of litterfall will be easily mixed with noises in the images. Therefore, it was difficult for these vegetation indices to capture the high variable dynamics of litterfall. Based on preliminary observation, finding a more sensitive index to capture the slight dynamics of litterfall and vegetation phenology is important in the future. Besides, using satellite images with higher temporal resolution could reduce the simultaneous influences of growth season and typhoon, and it was also useful to capture typhoon-induced litterfall. Overall, this study demonstrated the potential possibility of using remote sensing to assess the temporal dynamics of litterfall, which makes it possible to monitor the regional vegetation patterns in forest ecosystems.

4. REFERENCE

- Asner, G., Archer S., Hughes R., Ansley R., Wessman C. 2003 Net changes in regional woody vegetation cover and carbon storage in Texas drylands, 1937-1999. *Global Change Biology* 9: 316-335.
- Asner, G., Lobell D. 2000 A biogeophysical approach for automated SWIR unmixing of soils and vegetation. *Remote Sensing of Environment* 74:99-112.
- Barlow, J., Gardner T., Ferreira L., Peres C. 2007 Litter fall and decomposition in primary, secondary and plantation forests in the Brazilian Amazon. *Forest Ecology and Management* 247:91-97.
- Brown, S., Lugo A.E. 1982 The storage and production of organic matter in tropical forests and their role in the global carbon cycle. *Biotropica* 14:161-187.
- Chambers, J., Fisher J., Zeng H., Chapman E., Baker D., Hurtt G. 2007 Hurricane Katrina's carbon footprint on US Gulf Coast forests. *Science* 318:1107.
- Chang, S.C., Yeh C.F., Wu M.J., Hsia Y.J., Wu J.T. 2006 Quantifying fog water deposition by in situ exposure experiments in a mountainous coniferous forest in Taiwan. *Forest Ecology and Management* 224:11-18.
- Chapin, F., Matson P., Mooney H. 2002 *Principles of terrestrial ecosystem ecology*. Springer Verlag, New York.
- Chu, H.C. 2005 Estimation of nutrient storage and fluxes of litterfall in a yellow cypress forest ecosystem. National Dong Hwa University.
- DeFries, R. 2008 Terrestrial vegetation in the coupled human-earth system: Contributions of remote sensing. *Annual Review of Environment and Resources* 33:369-390.
- Drolet, G.G., Huemmrich K.F., Hall F.G., Middleton E.M., Black T.A., Barr A.G., Margolis H.A. 2005 A MODIS-derived photochemical reflectance index to detect inter-annual variations in the photosynthetic light-use efficiency of a boreal deciduous forest. *Remote Sensing of Environment* 98:212-224.
- Frolking, S., Palace M., Clark D., Chambers J., Shugart H., Hurtt G. 2009 Forest disturbance and recovery: A general review in the context of spaceborne remote sensing of impacts on aboveground biomass and canopy structure. *Journal of Geophysical Research* 114: G00E02.
- Garbulsky, M.F., Peñ Uelas J., Papale D., Filella I. 2008 Remote estimation of carbon dioxide uptake by a Mediterranean forest. *Global Change Biology* 14:2860-2867.
- Huete, A., Didan K., Miura T., Rodriguez E.P., Gao X., Ferreira L.G. 2002 Overview of the radiometric and biophysical performance of the MODIS vegetation indices. *Remote Sensing of Environment* 83:195-213.
- Irish, R., Barker J., Goward S., Arvidson T. 2006 Characterization of the Landsat-7 ETM automated cloud-cover assessment (ACCA) algorithm. *Photogrammetric engineering and remote sensing* 72:1179-1188.
- Liao, J., Wang H., Tsai C., Hseu Z. 2006 Litter production, decomposition and nutrient return of uplifted coral reef tropical forest. *Forest Ecology and Management* 235:174-185.
- Lin, K., Hamburg S., Tang S., Hsia Y., Lin T. 2003 Typhoon effects on litterfall in a subtropical forest. *Canadian Journal of Forest Research* 33:2184-2192.
- Lovett, G.M., Christenson L.M., Groffman P.M., Jones C.G., Hart J.E., Mitchell M.J. 2002 Insect Defoliation and Nitrogen Cycling in Forests. *BioScience* 52:335-341.
- Rahman, A.F., Gamon J.A., Fuentes D.A., Roberts D.A., Prentiss D. 2001 Modeling spatially distributed ecosystem flux of boreal forest using hyperspectral indices from AVIRIS imagery. *Journal of Geophysical Research* 106:33,579-33,591.
- Staelens, J., Nachtergale L., Luyssaert S., Lust N. 2003 A model of wind-influenced leaf litterfall in a mixed hardwood forest. *Canadian Journal of Forest Research* 33:201-209.
- Starr, M., Saarsalmi A., Hokkanen T., Merilä P., Helmisaari H.S. 2005 Models of litterfall production for Scots pine (*Pinus sylvestris* L.) in Finland using stand, site and climate factors. *Forest Ecology and Management* 205:215-225.
- Wang, H.C. 2009 Litterfall, litter decomposition and soil nutrients of natural and plantation forests in low elevation of central Taiwan. National Changhua University of Education.
- West, A.J., Lin C.W., Lin T.C., Hilton, R.G., Liu S.H., Chang C.T., Lin K.C., Galy A., Sparkes R.B., Hovius N. 2011 Mobilization and transport of coarse woody debris to the oceans triggered by an extreme tropical storm. *Limnology and Oceanography* 56:77-85.
- Whigham, D.F., Olmsted I., Cano E.C., Harmon M.E. 1991 The impact of hurricane Gilbert on trees, litterfall, and woody Debris in a dry tropical forest in the Northeastern Yucatan Peninsula. *Biotropica* 23:434-441.